Deliverable number: D3.3

DACOMAT - Damage Controlled Composite Materials

Report on mode II interface cohesive parameters using an improved single fibre fragmentation test

Bent F. Sørensen, The Technical University of Denmark

Deliverable details

Document name: D3.3 Report on mode II interface cohesive parameters using an improved single fibre fragmentation test

Responsible partner: DTU

Work package: WP3 - Materials Testing

Task: 3.1. Micromechanical testing

Due date: 31.12.2018

First delivery date: 05.03.2019

Final delivery date: 03.04.2019

Dissemination level	
X	PU = Public
	CO = Confidential, only for members of the consortium (including the EC)
	Classified, information as referred to in Commission Decision 2001/844/EC.
Deliverable type	
R	R: Document, report (excluding the periodic and final reports)
	DEM: Demonstrator, pilot, prototype, plan designs
	DEC: Websites, patents filing, press & media actions, videos, etc.
	OTHER: Software, technical diagram, etc.

Disclaimer:
The information in this document reflects the views only of the author, and the Commission cannot be held responsible for any use which may be made of the information contained therein.

The DACOMAT project has received funding from the European Union's Horizon 2020 research and innovation programme under GA No. 761072

1

1. Introduction

1.1. Motivation

Many large low-weight structures are made of composite materials since composite materials possess damage tolerance and good fatigue properties. Still, with yet larger and larger composite structure emerging, it is likewise of importance to develop new materials with yet improved damage tolerance and fatigue life. Since composite materials are complex, multi-scale materials, an efficient way of developing new materials is through tailoring the microscale properties (micromechanical optimization). For instance, a recent micromechanical model predicts that the in-plane fatigue limit of unidirectional fibre composites can be modified by optimizing the mechanical properties of the fibre/matrix interface (Sørensen and Goutianos, 2019). More specifically, the model predicts that a higher fatigue limit can be obtained by decreasing the debond energy and by increasing the frictional sliding shear stress. Thus, the interface should not "just be as strong as possible". Therefore, it is of high importance to use testing methods for characterizing the fibre/matrix interface that enables separation of debond energy and the frictional sliding shear stress. However, currently, there are no established testing methods and data analysis approaches that enable a clear determination of these parameters from microscale experiments.

A number of test methods involving a single filament embedded in matrix, such as single fibre pull-out, microbond test and single fibre fragmentation test (SFFT), have been used to characterize the mechanics of fibre/matrix interfaces in composites. An interesting approach for SFFT testing has been proposed by Kim and Nairn (2002). This approach involves the measurement of debond length as a function of the applied strain. This approach in principle enables the determination of both the debond energy and interfacial friction.

A number of theoretical models have been proposed for analyzing test data from single filament experiments. Typically, simpler models calculate a so called "interface strength" by dividing a maximum load by the interface area fractured, i.e. disregarding the debond energy.

Complicated models, on the other hand, model the interface in terms of both interface debond energy and friction, but typically involve lengthy mathematical equations due to the inclusion of Poisson's effects. For instance, analyzing the same data sets, two different advanced models (Kim and Nairn, 2002; Graciani et al., 2010) obtained a debond energy of 120 J/m^2 and 12 J/m^2 respectively, i.e. a difference in the order of a factor of ten. Due to the complexity of the models, it is difficult to evaluate which of the two numbers (120 J/m^2 or 12 J/m^2) describes the data better.

Recently, a more simple analysis has been published (Sørensen, 2017). In that model, which is only accurate when the debond length is about five time the fibre radius, an approach is described to determine fracture energy and frictional sliding shear stress in a manner similar to the way proposed by Kim and Nairn (2002). It also enables the determination of residual stresses from measurements of the opening displacements of the broken fibre ends. A major difference, however, is that for sufficiently long debond lengths, the model give a linear relationship between applied stress and debond length, so that the one parameter (debond energy) can be assessed by the interaction of a linear curve fit and the second parameter (frictional sliding shear stress) can be related directly to the slope of the line. This enables a quite direct assessment of parameters in comparison to the available experimental data and also allows quite direct assessment of upper and lower bounds of parameters.

1.2. Purpose

The purpose of the present work is to validate the approach proposed by Sørensen (2017), i.e., determine the debond energy and frictional sliding shear stress from measurements of consecutive measurements of applied stress and debond length, and aim to determine the residual stress from measurements of the opening displacement of the ends of a broken fibre.

The DACOMAT project has received funding from the European Union's Horizon 2020 research and innovation programme under GA No. 761072

3

2. Theoretical background

2.1 Micromechanical model results and test idea

The main idea utilized by the test is that once the debond length has exceeded a length corresponding to a few fibre radii, then (according to the model), the debond length ℓ_d will increase linearly with the applied stress, $\bar{\sigma}$. Mathematically this relationship can be written as (Sørensen, 2017):

$$\frac{\bar{\sigma}}{E_c} = \frac{\bar{\sigma}_i}{E_c} + 2\frac{\tau_s}{E_f}\left(\frac{\ell_d}{r}\right) \tag{2.1}$$

where $\bar{\sigma}_i$ is the so-called debond initiation stress given by

$$\frac{\bar{\sigma}_i}{E_c} = \frac{(1-V_f)E_m}{E_c}\Delta\varepsilon^T + 2\sqrt{\frac{(1-V_f)E_m}{E_c}\left(\frac{G_c^i}{E_f r}\right)} \tag{2.2}$$

In (2.1) the Young's modulus of the composite, E_c, is given by the rule of mixtures (Hull and Clyne, 1996),

$$E_c = V_f E_f + (1-V_f)E_m \tag{2.3}$$

where V_f is the fiber volume fraction, E_f and E_m are the Young's modulus of the fibre and matrix, respectively. The parameter $\Delta\varepsilon^T$ is an inelastic strain known as the misfit strain that controls the magnitude of residual stresses. $\Delta\varepsilon^T$ is defined to be zero at the stress-free state at the processing temperature. In the case of misfit strain originating from mismatch in the thermal expansion coefficients, it is given by

$$\Delta\varepsilon^T = (\alpha_f - \alpha_m)(T - T_0), \tag{2.4}$$

where α_f and α_m are the thermal expansion coefficients of the fibre and matrix, T_0 is the stress-free temperature (processing temperature) and T is the present temperature.

Further key parameters are τ_s, the frictional sliding shear stress acting along the debonded part of the fibre/matrix interface, G_c^i, the critical energy release rate (fracture energy) of the debond crack tip of the fiber/matrix interface and r, the fiber radius.
.

For single filament specimens in particular the fibre volume fraction is frequently very low, $V_f \approx 0$. The equations given above simplify further for $V_f \to 0$. First, from (2.3) we find that

$$E_c \to E_m \qquad for \quad V_f \to 0. \tag{2.5}$$

Then (2.1) reduces to

$$\frac{\overline{\sigma}}{E_m} = \Delta\varepsilon^T + 2\sqrt{\frac{\mathsf{G}_c^i}{E_f r}} + 2\frac{\tau_s}{E_f}\frac{\ell_d}{r}, \tag{2.6}$$

so that

$$\frac{d(\overline{\sigma}/E_m)}{d(\ell_d/r)} = 2\frac{\tau_s}{E_m} \qquad \Rightarrow \qquad \tau_s = \frac{E_f}{2}\frac{d(\overline{\sigma}/E_m)}{d(\ell_d/r)} \tag{2.7}$$

Furthermore, (2.2) reduces to

$$\frac{\overline{\sigma}_i}{E_m} = \Delta\varepsilon^T + 2\sqrt{\frac{\mathsf{G}_c^i}{E_f r}}. \tag{2.8}$$

Rewriting (2.8) leads to

$$\frac{\mathsf{G}_c^i}{E_f r} = \frac{1}{4}\left(\frac{\overline{\sigma}_i}{E_m} - \Delta\varepsilon^T\right)^2. \tag{2.9}$$

In the preset work we aim to identify the interface parameters τ_s and G_c^i from experimental data by the use of (2.7) and (2.9).

The idea is thus to measure related values of applied stress and debond length and to use the linear relationship predicted by the model to identify interface parameters.

2.2. Data analysis

In the present work, we pre-stress the fibres such that they will be stress-free at temperature T. Then, with $\Delta\varepsilon^T = 0$, the proposed analysis consists of two steps:

Step 1: First, $\bar{\sigma}$ is plotted as a function of ℓ_d. Since, according to (2.1) and (2.6), $\bar{\sigma}$ should depend linearly on ℓ_d, a straight line can be fitted to the data. This allows the determination of τ_s from the slope of the line according to (2.7).

Step 2: The value of G_c^i can be determined from $\bar{\sigma}_i$ by the use of (2.9), assuming that $\Delta\varepsilon^T$ is known or can be estimated form (2.4).

3. Experimental procedures

3.1 Specimen preparation

Single filament specimens were manufactured by casting a resin plate with embedded glass filaments between two glass plates in order to ensure smooth surfaces, such that the single fibre in the matrix could be observed by an optical microscope.

First, single glass fibres were extracted from a fibre bundle from a bobbin (HiPer tex W3030 from 3B) and cut into filaments of 42 cm in length. Each fibre was mounted on a horizontal glass plate at a special fixture inside a vacuum chamber. Each fibre was pre-loaded (5.7 grams) in order to keep them straight during the subsequent manufacturing steps. For each fibre, two small dots of glue (height about 1 mm) were placed near the edges of the bottom glass plate and after hardening of the glue, the fibre was placed on the glue dots with the pre-loads. Another (approximatively 1 mm high) glue dot was placed on the original glue dots so that the pre-stressed fibre was fixed to the dots about 1 mm above the bottom glass plate. A 2 mm high sealing (a standard epoxy glue), with a syringe acting as an inlet at the bottom, was placed around the left hand side, the right hand side and the bottom. Then the second glass plate was mounted, being parallel to the first glass plate. A spacer was used to ensure a

spacing of 2 mm between the two glass plates. The two glass plates and the sealings thus acted as an open mould (sealed at the sides and bottom) with pre-loaded fibres about 1 mm from both glass plates. The fixture with the mound was moved to a vacuum oven (MMM Group, type Vacucell 111) and the mould was tilted 45 degree, see Fig. 3.1.
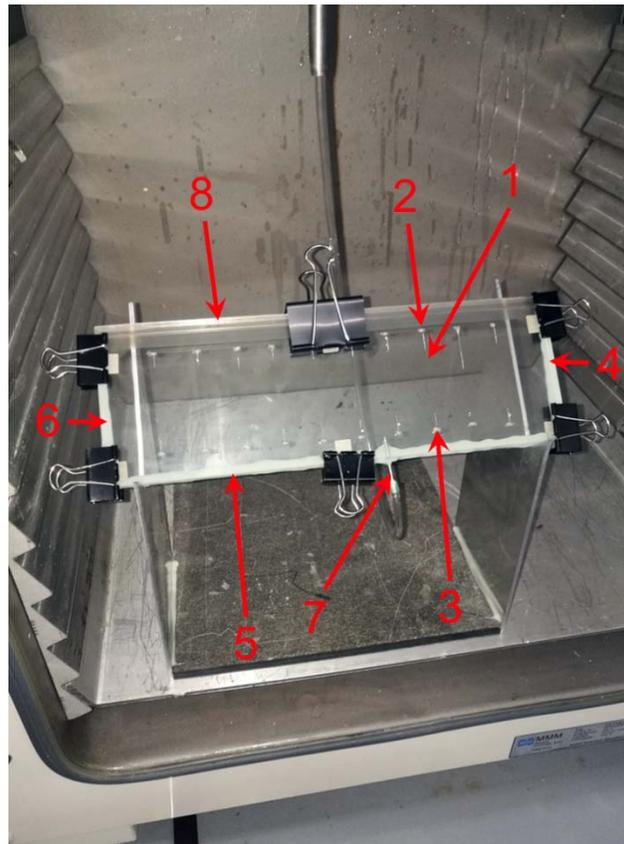
Fig. 3.1: Set-up for casting an epoxy plate with embedded fibres between two glass plates. A single fiber (1) is fixed at upper end (2) and lower end (3) in pre-stress state. The two glass plates are sealed at the right hand edge (4), bottom (5) and the left hand edge (6). A syringe (7) is used as inlet in the bottom of the mound.

Next, an epoxy resin (Araldite LY 1568) and hardener (Aradur 3489) were mixed in the ratio 100:28 and subsequently degassed in 95-155% vacuum for 5 minutes. A tube was connected from the resin box to syringe inlet in the bottom of the mould. The door to the vacuum chamber, in which the arrangement was mounted, was then closed and a low pressure (about 0.4 bars) was applied. The resin flow was then sucked into the tube, through the inlet and

The DACOMAT project has received funding from the European Union's Horizon 2020 research and innovation programme under GA No. 761072

7

slowly filled the mound from the bottom (Fig. 3.2). When the mound was filled the inlet tube was blocked, and the resin was cured (at 40°C for 24 hours, then 80°C for 6 hours) to form a solid resin plate with embedded filaments.
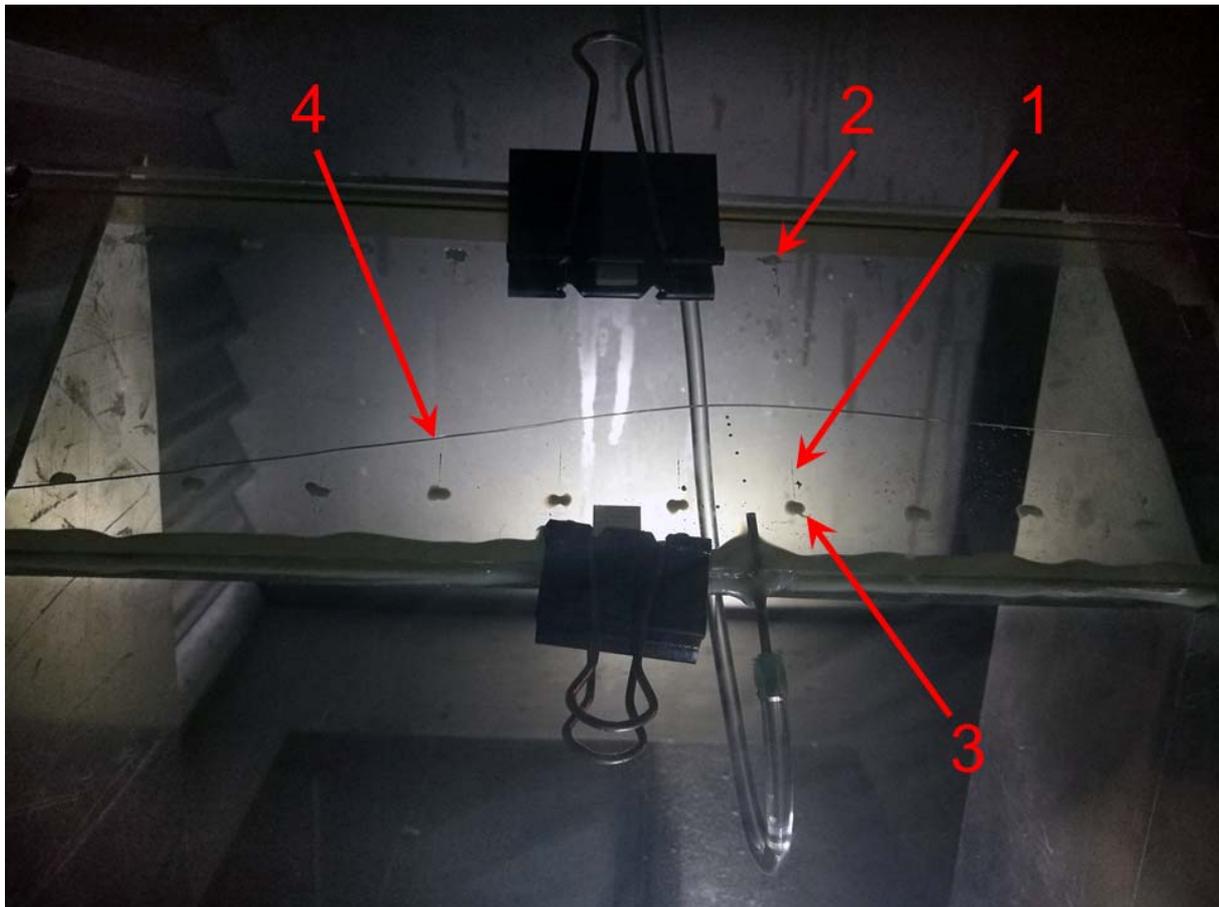
Fig. 3.2: Image of the infusion. The fibre (1) is fixed at its top end (2) and bottom end (3). The mound (space between the glass plates) is filled up from the bottom. The front of the resin is indicated (4).

After curing, the glass plates were disassembled and the resin plate was detached and placed in a CNC machine (QteC Isel GFV102/72-SW), where dog-bone shaped specimens were machined out with a single filament in each specimen. Nominal specimen dimensions are shown in Fig. 3.3.
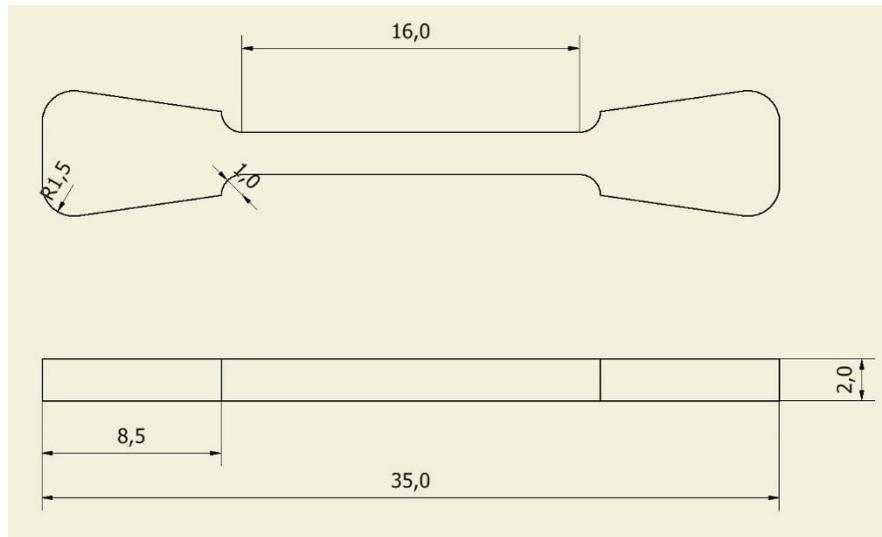
The DACOMAT project has received funding from the European Union's Horizon 2020 research and innovation programme under GA No. 761072

8

3.2 Test procedure

A specimen was mounted in a special 5kN loading device designed for tensile tension in both environmental scanning electron microscope and under an optical microscope. A load cell calibrated to 200 N was used. The experiments were conducted under displacement control. The loading device was designed such that the grips moved away symmetrically from the middle of the fixture. The displacement rate was controlled by an electrical motor, controlled via a joy stick connected to a control program (JVL Motor Control Systems). Data (elapsed time and load cell output) were collected at 10 Hz on a PC using a Daisylab program (version 9.0). An x-y-z coordinate system was used to describe locations on the specimen.

The loading device was mounted to the x-y-z stage of a DeltaPix microscope system. A DeltaPix Insight (version 4.0.9) software program was used for acquiring digital images. Images were recorded at a magnification of 200 times using a resolution of 1616 by 1216 pixels. Light setting from both below and above was used. A polarization filter, placed between the specimen and camera, was also used. An image of the work space is shown in Fig. 3.4. Fig. 3.5 shows a close up of the specimen just mounted in the grips, and Fig. 3.6 shows the specimen fixed in both grips.

The DACOMAT project has received funding from the European Union's Horizon 2020 research and innovation programme under GA No. 761072

9

After mounting of the specimen in the loading device, the coordinate of the edges and ends of the gauge section of the specimen were noted down. The location of the filament was found next.
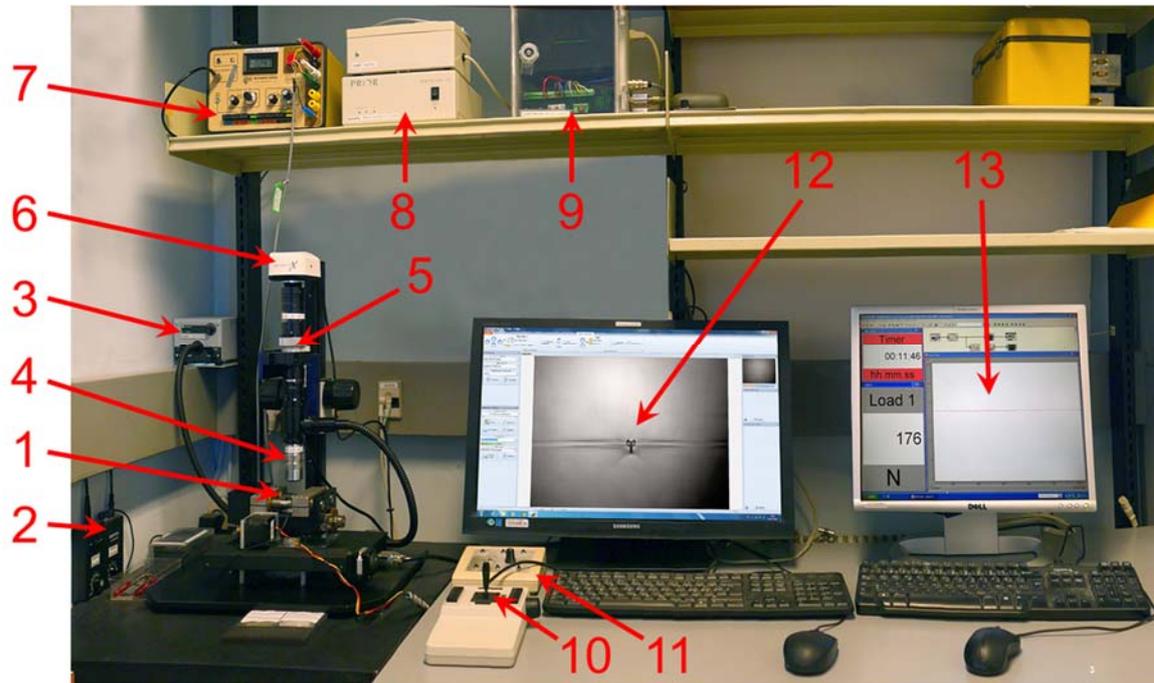
Fig. 3.4: Overview of test set-up. The dog-bone specimen is mounted in the 5-kN tensile test rig (1). There are controls for light from below (2) and from above (3). Light from the specimen goes through the camera lens (4) and the polar filter (5) that can be turned continuously, to the digital camera (6). Load amplifier (7) for the strain gauges load cell. The control (8) for the x-y-z stage positioning test rig (1). The test rig loading motor control system (9) is operated by a joy-stick (10) via a test-rig load-motor control box (11). The microscope image is shown live on the screen (12). Load-time data is shown on a separate PC screen (13).
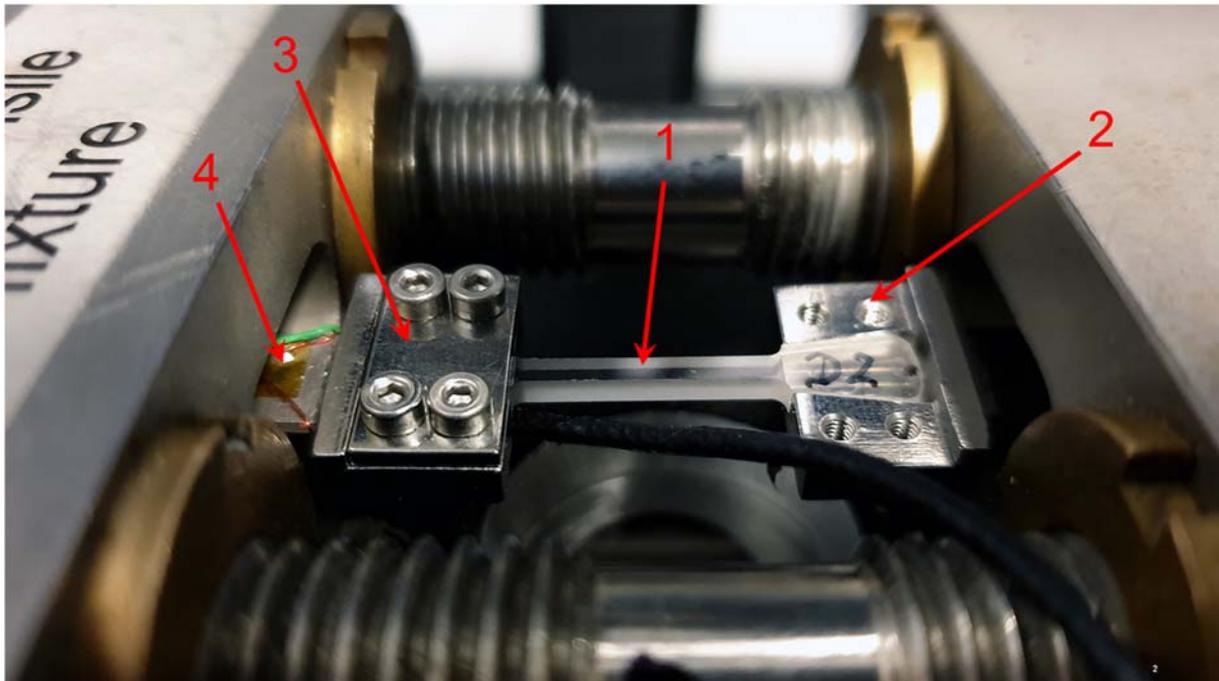
Fig. 3.5: Close-up of the test specimen (1) placed in the grips. The right hand grip (2) is open, so that the specimen can be seen. The left hand grip (3) is closed. Four strain gauges (4), coupled as a full Wheatstone bridge, act as a load cell.
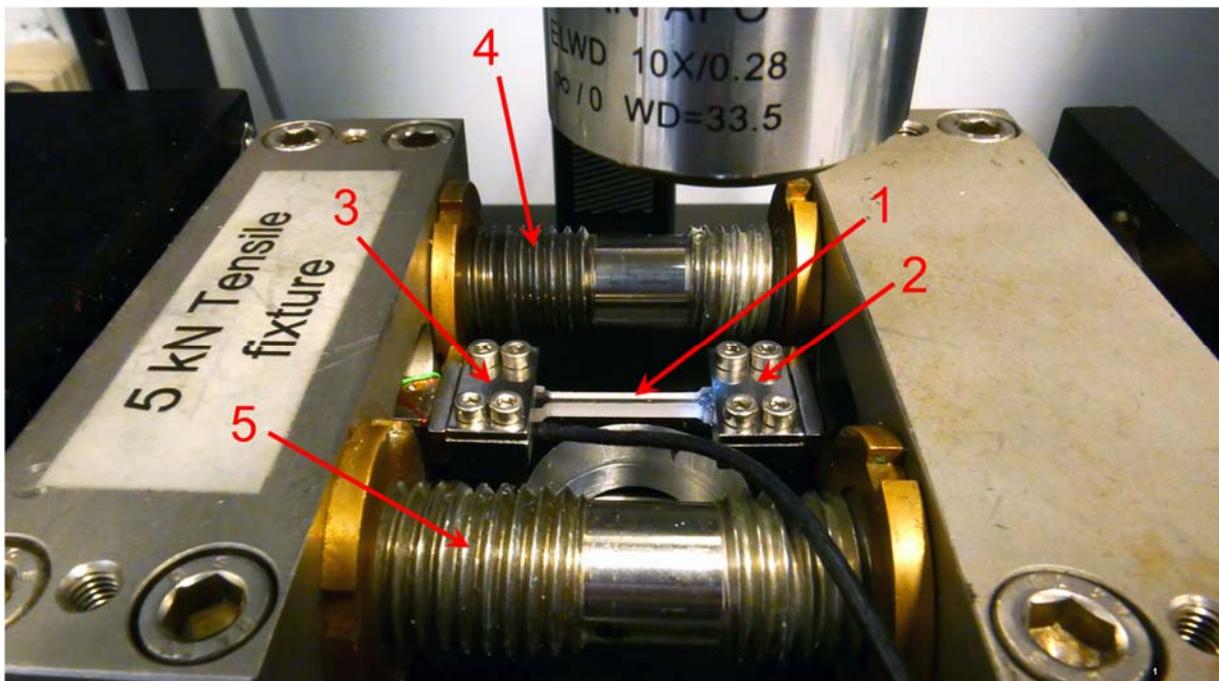
Fig. 3.6: Image of the test specimen (1) mounted at the right hand (2) and left hand (3) grips - ready for testing. Displacement of the sample achieved by controlling the columns (4) and (5).

The DACOMAT project has received funding from the European Union's Horizon 2020 research and innovation programme under GA No. 761072

11

The loading procedure was as follows. The data acquisition program was started. The motor was activated. Loading continued until pre-selected load levels. When the load level was reached, the motor direction was reversed and the specimen was unloaded by 15-20 N. Thereafter, the displacement was held fixed. Next, the fibre was "scanned" for fibre breakage by translating the stage, so that the fibre could be observed along the entire length within the gauge section. In case a fibre fracture was found, images were recorded (to document the debond length) and its x-y-z coordinate was noted down, so that later the history of each fibre breakage could be established. Details (use of light sources, filter etc.) were noted down for each image recorded. After the entire fibre length had been investigated the specimen was loaded to the next load level and the process described was repeated..

4. Experimental results

4.1. Observations

Fig. 4.1 and Fig. 4.2. show images of a broken fibre and the associated debond zone (applied strain 2.1%) under different light and polarisation conditions. For both images, the locus of fibre breakage appears as black and the colour change along the fibre/matrix interface is taken to be the debond length. Debond length can be identified at four locations: along the upper and lower interface to the right hand side of the fibre break and along the upper and lower interface to the left hand side of the fibre break.

Fig. 4.3 shows the same fibre at a higher applied strain (2.4%). In comparison with Fig. 4.1, the debond length has clearly increased. Again, four slightly different debond lengths can be identified.
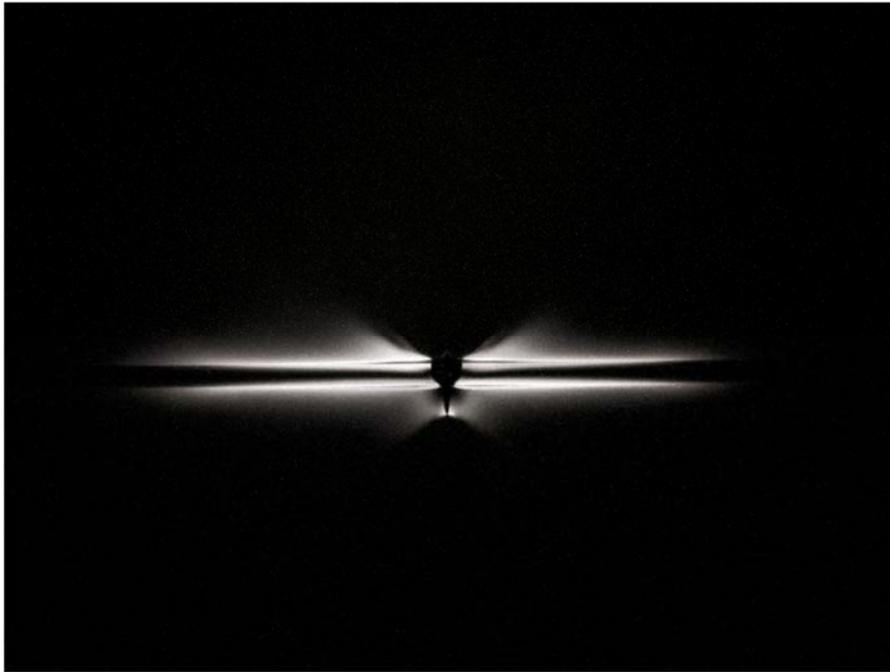
Fig. 4.1: Image of a broken and debonded fibre obtained using top light only and a polarised filter (2.1% strain). Fibre diameter is 16 microns.
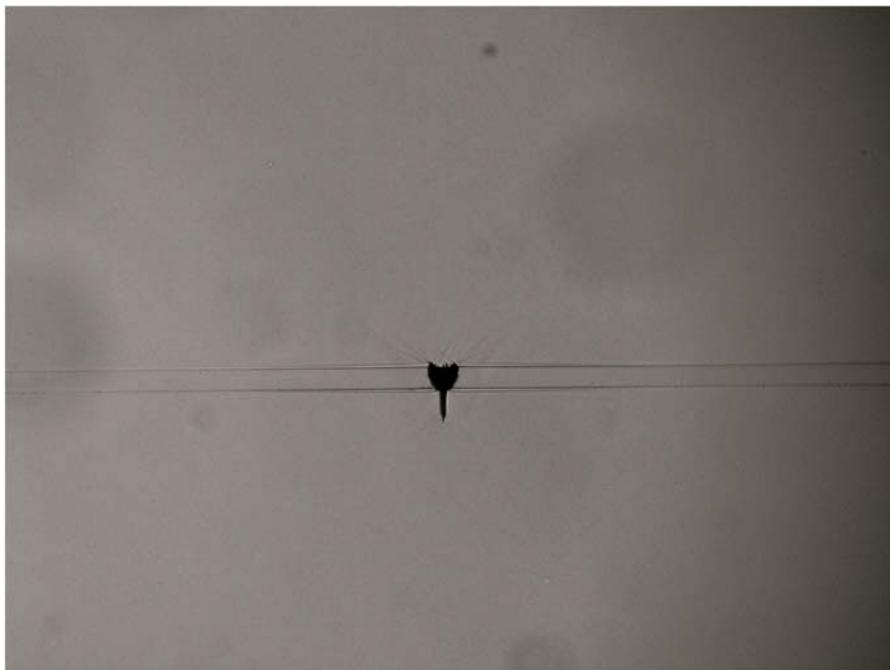
Fig. 4.2: Image of a broken and debonded fibre obtained using bottom and top light (2.1% strain). Same fibre break as in Fig. 4.1.

The DACOMAT project has received funding from the European Union's Horizon 2020 research and innovation programme under GA No. 761072

13
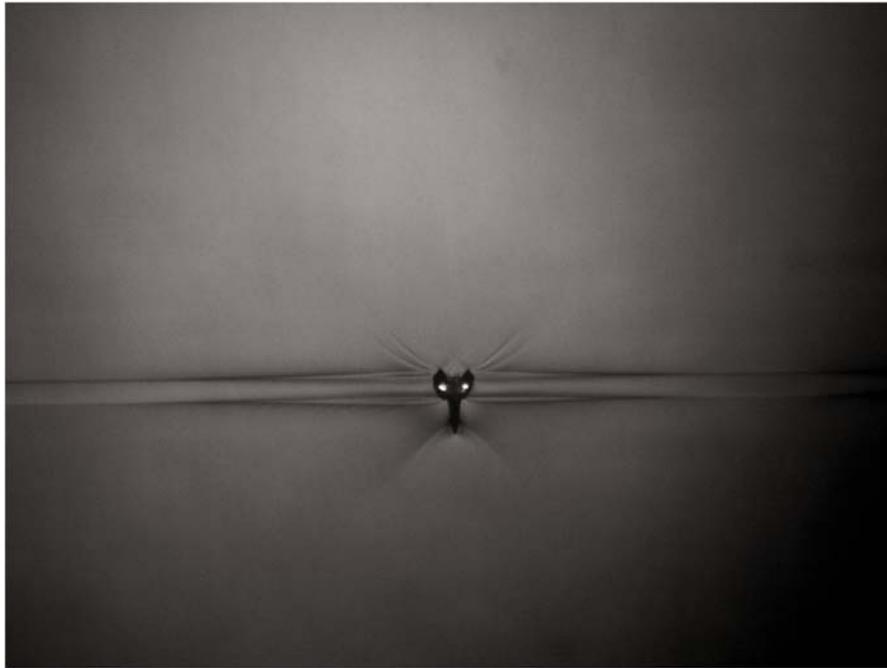
Fig. 4.3: Image of the same broken and debonded fibre as in Fig. 4.1 and Fig. 4.2, but at at higher strain (2.4% strain). Image was obtained using bottom and top light.

4.2. Interface parameters

Fig. 4.4 shows the relationship between the debond length, normalized by the fibre radius and the applied stress, normalized by the composite stiffness. A straight line is fitted to the data. From the slope of the line, the frictional sliding shear stress is calculated to be 66 MPa using (2.7) and material data given in Table 1. Reading off the normalized debond initiation stress to be 0.013. Then, ignoring residual stresses (setting the mismatch strain equal to zero) we calculate the debond energy from (2.9) to be 24 J/m^2. These values are comparable to those found in the literature for similar materials systems (Kim and Nairn, 2002; Sørensen, 2017).

Table 1: Material parameters

Fibre stiffness, E_f	70 GPa
Matrix stiffness, E_m	3 GPa
Fibre radius, r	8 μm

The DACOMAT project has received funding from the European Union's Horizon 2020 research and innovation programme under GA No. 761072

14

SFFT_D2_1f.opj
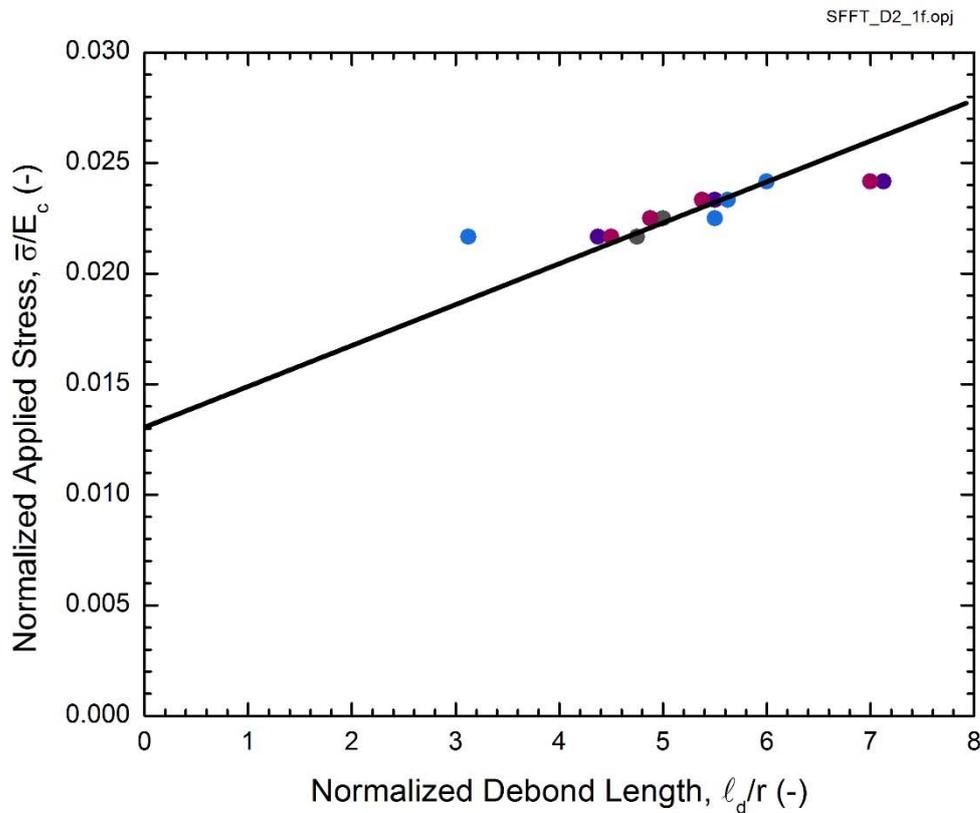
Fig. 4.4: Relationship between measured debond length and applied stress (both normalized). Circles are experimental measurements. A linear regression line, used to estimate interface parameters, is also shown.

5. Summary and conclusions

A modified single filament testing method for the determination of debond energy and frictional sliding shear stress has been validated. A material system (glass fibre in an epoxy matrix) was tested. The debond length was recorded as a function of the applied strain level and analysed using a micromechanical model. From the analysis of the experimental data, the frictional sliding shear stress was found to be 66 MPa and the debond energy was calculated to be 23 J/m^2. The testing approach can henceforward be used to characterize new fibre sizings (coatings) and thus separate effects of chemistry (debond energy) and roughness

The DACOMAT project has received funding from the European Union's Horizon 2020 research and innovation programme under GA No. 761072

15

(frictional sliding shear stress). This will be useful for development of future composite materials.

Acknowledgements

Thanks to Jonas Heininge for specimen manufacture, thanks to Adnan Bijedic for specimen cutting, and Erik Vogeley for setting up the testing device and running the experiments and Hans Lilholt for discussions during this work. Thanks to Peter Jenkins for proof-reading the report.

References

Graciani, E., Varna, J., Mantic, V., Blazquez, A. and Paris, F., 2011. "Evaluation of interfacial fracture toughness and friction coefficient in the single fiber fragmentation test". *Procedia Engineering*. 10, pp. 2478-83.

Hull, D., and Clyne, T. W., 1996, An Introduction to Composite Materials, second edition, Cambridge University Press, p. 62.

Kim, B. W., Nairn, J. A., 2002. "Observations of fiber fracture and interfacial debonding phenomena using the fragmentation tests in single fiber composites". *Journal of Composite Materials*. 36, pp. 1825-58.

Sørensen, B.F., 2017, "Micromechanical model of the single fiber fragmentation test", Mechanics of Materials, Vol. 104, pp. 38-48.

Sørensen, B. F, and Goutianos S., 2019, "Micromechanical model for prediction of the fatigue limit for unidirectional fibre composites", *Mechanics of Materials*, Vol. 131, pp. 169-87.

The DACOMAT project has received funding from the European Union's Horizon 2020 research and innovation programme under GA No. 761072

16